EUROPEAN LABORATORY FOR PARTICLE PHYSICS

CERN-PPE/97-064
5 June 1997

An Updated Study of B Meson Oscillations using Dilepton Events

The OPAL Collaboration

Abstract

This paper reports a study of B meson oscillations using hadronic Z^0 decays with two identified leptons, and updates a previous publication by including data collected in 1994. Decay times are reconstructed for each of the semileptonic B decays by forming vertices which include the lepton and by estimating the B meson momentum. The mass difference, Δm_{d}, between the two mass eigenstates in the $\mathrm{B}^0_{\mathrm{d}}$ system is measured to be $0.430 \pm 0.043\ ^{+0.028}_{-0.030}\ \mathrm{ps}^{-1}$, where the first error is statistical and the second error is systematic. For the $\mathrm{B}^0_{\mathrm{s}}$ system, a lower limit of $\Delta m_{\mathrm{s}} > 2.2\ \mathrm{ps}^{-1}$ is obtained at 95% C.L.

(To be submitted to Zeitschrift für Physik C)

The OPAL Collaboration

K. Ackerstaff[8], G. Alexander[23], J. Allison[16], N. Altekamp[5], K.J. Anderson[9], S. Anderson[12], S. Arcelli[2], S. Asai[24], D. Axen[29], G. Azuelos[18,a], A.H. Ball[17], E. Barberio[8], R.J. Barlow[16], R. Bartoldus[3], J.R. Batley[5], S. Baumann[3], J. Bechtluft[14], C. Beeston[16], T. Behnke[8], A.N. Bell[1], K.W. Bell[20], G. Bella[23], S. Bentvelsen[8], P. Berlich[10], S. Bethke[14], O. Biebel[14], A. Biguzzi[5], S.D. Bird[16], V. Blobel[27], I.J. Bloodworth[1], J.E. Bloomer[1], M. Bobinski[10], P. Bock[11], D. Bonacorsi[2], M. Boutemeur[34], B.T. Bouwens[12], S. Braibant[12], L. Brigliadori[2], R.M. Brown[20], H.J. Burckhart[8], C. Burgard[8], R. Bürgin[10], P. Capiluppi[2], R.K. Carnegie[6], A.A. Carter[13], J.R. Carter[5], C.Y. Chang[17], D.G. Charlton[1,b], D. Chrisman[4], P.E.L. Clarke[15], I. Cohen[23], J.E. Conboy[15], O.C. Cooke[16], M. Cuffiani[2], S. Dado[22], C. Dallapiccola[17], G.M. Dallavalle[2], S. De Jong[12], L.A. del Pozo[4], K. Desch[3], M.S. Dixit[7], E. do Couto e Silva[12], M. Doucet[18], E. Duchovni[26], G. Duckeck[34], I.P. Duerdoth[16], D. Eatough[16], J.E.G. Edwards[16], P.G. Estabrooks[6], H.G. Evans[9], M. Evans[13], F. Fabbri[2], M. Fanti[2], A.A. Faust[30], F. Fiedler[27], M. Fierro[2], H.M. Fischer[3], I. Fleck[8], R. Folman[26], D.G. Fong[17], M. Foucher[17], H. Fukui[24], A. Fürtjes[8], D.I. Futyan[16], P. Gagnon[7], J.W. Gary[4], J. Gascon[18], S.M. Gascon-Shotkin[17], N.I. Geddes[20], C. Geich-Gimbel[3], T. Geralis[20], G. Giacomelli[2], P. Giacomelli[4], R. Giacomelli[2], V. Gibson[5], W.R. Gibson[13], D.M. Gingrich[30,a], D. Glenzinski[9], J. Goldberg[22], M.J. Goodrick[5], W. Gorn[4], C. Grandi[2], E. Gross[26], J. Grunhaus[23], M. Gruwé[8], C. Hajdu[32], G.G. Hanson[12], M. Hansroul[8], M. Hapke[13], C.K. Hargrove[7], P.A. Hart[9], C. Hartmann[3], M. Hauschild[8], C.M. Hawkes[5], R. Hawkings[27], R.J. Hemingway[6], M. Herndon[17], G. Herten[10], R.D. Heuer[8], M.D. Hildreth[8], J.C. Hill[5], S.J. Hillier[1], T. Hilse[10], P.R. Hobson[25], R.J. Homer[1], A.K. Honma[28,a], D. Horváth[32,c], R. Howard[29], D.E. Hutchcroft[5], P. Igo-Kemenes[11], D.C. Imrie[25], M.R. Ingram[16], K. Ishii[24], A. Jawahery[17], P.W. Jeffreys[20], H. Jeremie[18], M. Jimack[1], A. Joly[18], C.R. Jones[5], G. Jones[16], M. Jones[6], U. Jost[11], P. Jovanovic[1], T.R. Junk[8], D. Karlen[6], V. Kartvelishvili[16], K. Kawagoe[24], T. Kawamoto[24], R.K. Keeler[28], R.G. Kellogg[17], B.W. Kennedy[20], J. Kirk[29], A. Klier[26], S. Kluth[8], T. Kobayashi[24], M. Kobel[10], D.S. Koetke[6], T.P. Kokott[3], M. Kolrep[10], S. Komamiya[24], T. Kress[11], P. Krieger[6], J. von Krogh[11], P. Kyberd[13], G.D. Lafferty[16], R. Lahmann[17], W.P. Lai[19], D. Lanske[14], J. Lauber[15], S.R. Lautenschlager[31], J.G. Layter[4], D. Lazic[22], A.M. Lee[31], E. Lefebvre[18], D. Lellouch[26], J. Letts[12], L. Levinson[26], S.L. Lloyd[13], F.K. Loebinger[16], G.D. Long[28], M.J. Losty[7], J. Ludwig[10], A. Macchiolo[2], A. Macpherson[30], M. Mannelli[8], S. Marcellini[2], C. Markus[3], A.J. Martin[13], J.P. Martin[18], G. Martinez[17], T. Mashimo[24], P. Mättig[3], W.J. McDonald[30], J. McKenna[29], E.A. Mckigney[15], T.J. McMahon[1], R.A. McPherson[8], F. Meijers[8], S. Menke[3], F.S. Merritt[9], H. Mes[7], J. Meyer[27], A. Michelini[2], G. Mikenberg[26], D.J. Miller[15], A. Mincer[22,e], R. Mir[26], W. Mohr[10], A. Montanari[2], T. Mori[24], M. Morii[24], U. Müller[3], K. Nagai[26], I. Nakamura[24], H.A. Neal[8], B. Nellen[3], R. Nisius[8], S.W. O'Neale[1], F.G. Oakham[7], F. Odorici[2], H.O. Ogren[12], N.J. Oldershaw[16], M.J. Oreglia[9], S. Orito[24], J. Pálinkás[33,d], G. Pásztor[32], J.R. Pater[16], G.N. Patrick[20], J. Patt[10], M.J. Pearce[1], S. Petzold[27], P. Pfeifenschneider[14], J.E. Pilcher[9], J. Pinfold[30], D.E. Plane[8], P. Poffenberger[28], B. Poli[2], A. Posthaus[3], H. Przysiezniak[30], D.L. Rees[1], D. Rigby[1], S. Robertson[28], S.A. Robins[22], N. Rodning[30], J.M. Roney[28], A. Rooke[15], E. Ros[8], A.M. Rossi[2], M. Rosvick[28], P. Routenburg[30], Y. Rozen[22], K. Runge[10], O. Runolfsson[8], U. Ruppel[14], D.R. Rust[12], R. Rylko[25], K. Sachs[10], T. Saeki[24], E.K.G. Sarkisyan[23], C. Sbarra[29], A.D. Schaile[34], O. Schaile[34], F. Scharf[3], P. Scharff-Hansen[8], P. Schenk[34], J. Schieck[11], P. Schleper[11], B. Schmitt[8], S. Schmitt[11], A. Schöning[8], M. Schröder[8], H.C. Schultz-Coulon[10], M. Schulz[8], M. Schumacher[3], C. Schwick[8], W.G. Scott[20], T.G. Shears[16], B.C. Shen[4], C.H. Shepherd-Themistocleous[8], P. Sherwood[15], G.P. Siroli[2], A. Sittler[27], A. Skillman[15],

A. Skuja[17], A.M. Smith[8], G.A. Snow[17], R. Sobie[28], S. Söldner-Rembold[10], R.W. Springer[30], M. Sproston[20], K. Stephens[16], J. Steuerer[27], B. Stockhausen[3], K. Stoll[10], D. Strom[19], P. Szymanski[20], R. Tafirout[18], S.D. Talbot[1], S. Tanaka[24], P. Taras[18], S. Tarem[22], R. Teuscher[8], M. Thiergen[10], M.A. Thomson[8], E. von Törne[3], S. Towers[6], I. Trigger[18], E. Tsur[23], A.S. Turcot[9], M.F. Turner-Watson[8], P. Utzat[11], R. Van Kooten[12], M. Verzocchi[10], P. Vikas[18], E.H. Vokurka[16], H. Voss[3], F. Wäckerle[10], A. Wagner[27], C.P. Ward[5], D.R. Ward[5], P.M. Watkins[1], A.T. Watson[1], N.K. Watson[1], P.S. Wells[8], N. Wermes[3], J.S. White[28], B. Wilkens[10], G.W. Wilson[27], J.A. Wilson[1], G. Wolf[26], T.R. Wyatt[16], S. Yamashita[24], G. Yekutieli[26], V. Zacek[18], D. Zer-Zion[8]

[1]School of Physics and Space Research, University of Birmingham, Birmingham B15 2TT, UK
[2]Dipartimento di Fisica dell' Università di Bologna and INFN, I-40126 Bologna, Italy
[3]Physikalisches Institut, Universität Bonn, D-53115 Bonn, Germany
[4]Department of Physics, University of California, Riverside CA 92521, USA
[5]Cavendish Laboratory, Cambridge CB3 0HE, UK
[6] Ottawa-Carleton Institute for Physics, Department of Physics, Carleton University, Ottawa, Ontario K1S 5B6, Canada
[7]Centre for Research in Particle Physics, Carleton University, Ottawa, Ontario K1S 5B6, Canada
[8]CERN, European Organisation for Particle Physics, CH-1211 Geneva 23, Switzerland
[9]Enrico Fermi Institute and Department of Physics, University of Chicago, Chicago IL 60637, USA
[10]Fakultät für Physik, Albert Ludwigs Universität, D-79104 Freiburg, Germany
[11]Physikalisches Institut, Universität Heidelberg, D-69120 Heidelberg, Germany
[12]Indiana University, Department of Physics, Swain Hall West 117, Bloomington IN 47405, USA
[13]Queen Mary and Westfield College, University of London, London E1 4NS, UK
[14]Technische Hochschule Aachen, III Physikalisches Institut, Sommerfeldstrasse 26-28, D-52056 Aachen, Germany
[15]University College London, London WC1E 6BT, UK
[16]Department of Physics, Schuster Laboratory, The University, Manchester M13 9PL, UK
[17]Department of Physics, University of Maryland, College Park, MD 20742, USA
[18]Laboratoire de Physique Nucléaire, Université de Montréal, Montréal, Quebec H3C 3J7, Canada
[19]University of Oregon, Department of Physics, Eugene OR 97403, USA
[20]Rutherford Appleton Laboratory, Chilton, Didcot, Oxfordshire OX11 0QX, UK
[22]Department of Physics, Technion-Israel Institute of Technology, Haifa 32000, Israel
[23]Department of Physics and Astronomy, Tel Aviv University, Tel Aviv 69978, Israel
[24]International Centre for Elementary Particle Physics and Department of Physics, University of Tokyo, Tokyo 113, and Kobe University, Kobe 657, Japan
[25]Brunel University, Uxbridge, Middlesex UB8 3PH, UK
[26]Particle Physics Department, Weizmann Institute of Science, Rehovot 76100, Israel
[27]Universität Hamburg/DESY, II Institut für Experimental Physik, Notkestrasse 85, D-22607 Hamburg, Germany
[28]University of Victoria, Department of Physics, P O Box 3055, Victoria BC V8W 3P6, Canada
[29]University of British Columbia, Department of Physics, Vancouver BC V6T 1Z1, Canada
[30]University of Alberta, Department of Physics, Edmonton AB T6G 2J1, Canada

[31]Duke University, Dept of Physics, Durham, NC 27708-0305, USA
[32]Research Institute for Particle and Nuclear Physics, H-1525 Budapest, P O Box 49, Hungary
[33]Institute of Nuclear Research, H-4001 Debrecen, P O Box 51, Hungary
[34]Ludwigs-Maximilians-Universität München, Sektion Physik, Am Coulombwall 1, D-85748 Garching, Germany

[a] and at TRIUMF, Vancouver, Canada V6T 2A3
[b] and Royal Society University Research Fellow
[c] and Institute of Nuclear Research, Debrecen, Hungary
[d] and Department of Experimental Physics, Lajos Kossuth University, Debrecen, Hungary
[e] and Depart of Physics, New York University, NY 1003, USA

1 Introduction

In the Standard Model, a second-order weak transition transforms neutral B mesons into their antiparticles [1]. The neutral B mesons therefore oscillate between particle and antiparticle states before decaying. The frequency of the oscillation depends on the top quark mass, the Cabibbo-Kobayashi-Maskawa matrix elements, and meson decay constants. By analogy with the K^0 case and neglecting CP violation, the mass eigenstates, $|\mathrm{B}_1\rangle$ and $|\mathrm{B}_2\rangle$, of B^0_q (q=d or s) can be described as follows:

$$
\begin{aligned}
|\mathrm{B}_1\rangle &= \frac{1}{\sqrt{2}}(|\mathrm{B}^0_\mathrm{q}\rangle + |\bar{\mathrm{B}}^0_\mathrm{q}\rangle), \\
|\mathrm{B}_2\rangle &= \frac{1}{\sqrt{2}}(|\mathrm{B}^0_\mathrm{q}\rangle - |\bar{\mathrm{B}}^0_\mathrm{q}\rangle).
\end{aligned}
$$

If a B^0_q is produced at time $t = 0$, the probabilities of having a B^0_q or a $\bar{\mathrm{B}}^0_\mathrm{q}$ at proper time t are[1]

$$
\begin{aligned}
P_{\mathrm{B}^0_\mathrm{q}}(t) &= \frac{1}{\tau}e^{-t/\tau}\ \cos^2\left(\frac{\Delta m_\mathrm{q}\, t}{2}\right) \\
P_{\bar{\mathrm{B}}^0_\mathrm{q}}(t) &= \frac{1}{\tau}e^{-t/\tau}\ \sin^2\left(\frac{\Delta m_\mathrm{q}\, t}{2}\right)
\end{aligned}
$$

where τ is the B^0_q lifetime. The frequency of the oscillation is given by Δm_q, the mass difference of the two mass eigenstates ($\Delta m_\mathrm{q} = m_{\mathrm{B}_1} - m_{\mathrm{B}_2}$). For $\mathrm{B}^0_\mathrm{d} - \bar{\mathrm{B}}^0_\mathrm{d}$ mixing, time-integrated measurements from ARGUS and CLEO give $x_\mathrm{d} = \Delta m_\mathrm{d}\,\tau = 0.67 \pm 0.08$ [2, 3]. Published measurements of the frequency of $\mathrm{B}^0_\mathrm{d} - \bar{\mathrm{B}}^0_\mathrm{d}$ oscillations made at LEP are available using several different techniques [4, 5, 6, 7, 8]. Lower limits on Δm_s have been reported by the ALEPH [8, 9] and the OPAL [6, 7] collaborations.

Extracting information on CKM matrix elements from the measurements of Δm_d and Δm_s is prone to large uncertainties due to poorly known meson decay constants. These uncertainties can be reduced by considering the ratio $\Delta m_\mathrm{s}/\Delta m_\mathrm{d}$. Given the present knowledge of V_ts and V_td one expects Δm_s to be of the order of 10 ps^{-1} [10]. Using dilepton events in data collected between 1991 and 1993 [6], we studied $\mathrm{B}^0_\mathrm{d} - \bar{\mathrm{B}}^0_\mathrm{d}$ and $\mathrm{B}^0_\mathrm{s} - \bar{\mathrm{B}}^0_\mathrm{s}$ oscillations, reporting $\Delta m_\mathrm{d} = 0.462\ ^{+0.040}_{-0.053}\ ^{+0.052}_{-0.035}\ \mathrm{ps}^{-1}$ and $\Delta m_\mathrm{s} > 2.2\ \mathrm{ps}^{-1}$ at 95% C.L. We update these results by including data collected in 1994. The technique is the same as that reported previously [6]. Hadronic Z^0 decays with two lepton candidates, one in each thrust hemisphere, are selected. The reconstruction of a secondary vertex that includes the lepton is attempted for each lepton candidate, yielding an estimate of the decay length of the b hadron. This is combined with an estimate of the relativistic boost of the b hadron to give the proper decay time. The likelihood of each event is calculated as a function of Δm_d and Δm_s according to the measured proper times and the charge combination of the two leptons. The result for Δm_d and the lower limit on Δm_s are then obtained using a maximum likelihood technique.

[1] The contribution of $\Delta\Gamma$, the difference between the total decay widths of the mass eigenstates, to the oscillations is expected to be negligible and has been ignored.

2 Event Selection and Simulation

2.1 Event Selection

The analysis is performed on data collected by OPAL in the vicinity of the Z^0 peak from 1991 to 1994. The OPAL detector has been described elsewhere [11, 12]. Hadronic Z^0 decays are selected using criteria described in [13]. A cone jet algorithm [14] is used to classify tracks and electromagnetic clusters not associated to tracks into jets. The size of the cone is chosen so as to include nearly all the decay products of a b hadron into one jet. The jets also include particles produced in the fragmentation process, which originate from the e^+e^- collision point. A total of 2 874 660 hadronic events satisfy the event selection criteria.

Electrons are identified using an artificial neural network [6] which is trained on a sample of simulated hadronic Z^0 decays. Electrons from photon conversions are rejected as in [15]. Muons are identified as in [16]. Lepton candidates are required to satisfy $p > 2.0\,\mathrm{GeV}$ and $|\cos\theta| < 0.9$. Additional kinematic criteria are imposed to reduce the fraction of leptons in the sample coming from cascade decays of the type $\mathrm{b} \to \mathrm{c} \to \ell$.

The techniques for secondary vertex reconstruction and proper time estimation are described in [6]. Dilepton events with at least one reconstructed vertex are selected.

2.2 Event Simulation

Monte Carlo events are used to predict the relative abundances and decay time distributions for lepton candidates from various physics processes. The JETSET 7.4 Monte Carlo program [17] with parameters tuned to OPAL data [18] is used to generate $Z^0 \to \mathrm{q\overline{q}}$ events which are processed by the detector simulation program [19]. The fragmentation of b and c quarks is parametrised using the fragmentation function of Peterson *et al.* [20], with $\langle x_E \rangle$ for b and c hadrons given by the central values in Table 1.

Quantity	Value
$\langle x_E \rangle_b$	0.697 ± 0.013 [16]
$\langle x_E \rangle_c$	0.51 ± 0.02 [15]
$B(\mathrm{b} \to \ell)$	$(10.5 \pm 0.6 \pm 0.5)\%$ [16]
$B(\mathrm{b} \to \mathrm{c} \to \ell)$	$(7.7 \pm 0.4 \pm 0.7)\%$ [16]
$B(\mathrm{b} \to \bar{\mathrm{c}} \to \ell)$	$(1.3 \pm 0.5)\%$ [16]
$M(\mathrm{B_s^0})$	5.48 GeV
$M(\Lambda_\mathrm{b})$	5.62 GeV
$\tau_{\mathrm{B^+}}/\tau_{\mathrm{B_d^0}}$	1.03 ± 0.06 [3]
$\tau_{\mathrm{B_s^0}}/\tau_{\mathrm{B_d^0}}$	1.03 ± 0.08 [3]
$\tau_{\Lambda_\mathrm{b}}/\tau_{\mathrm{B_d^0}}$	0.73 ± 0.06 [3]
$\langle \tau_\mathrm{b} \rangle$	1.55 ± 0.02 ps [3]

Table 1: The parameters used for the Monte Carlo simulation.

Standard Model values of the partial widths of the Z^0 into $q\overline{q}$ are used [21]. The mixture of c-flavoured hadrons produced both in $Z^0 \to c\overline{c}$ events and in b hadron decays is as prescribed in [15]. The semileptonic branching ratios of charm hadrons and associated uncertainties are also those of [15]. The central values in Table 1 are taken for the inclusive branching ratios for $b \to \ell$, $b \to c \to \ell$ and $b \to \overline{c} \to \ell$. The semileptonic branching ratios of the individual b hadrons are assumed to be proportional to the lifetimes. The models used in describing the semileptonic decays of b and c hadrons are those used in determining the central values in [15]. The asssumed masses for B_s^0 and Λ_b particles are also given in Table 1. The lifetimes of b hadrons used in this analysis were taken from the world average values [3], as indicated in Table 1.

3 Fit Results for Δm_d

The numbers of dilepton events with at least one secondary vertex constructed for the combination of e-e, e-μ and μ-μ, are listed in Table 2, separately for like-sign and unlike-sign dilepton events. Also included is the total number of secondary vertices reconstructed in these events.

	e-e	e-μ	μ-μ	total	total vertices
unlike-sign	891	1791	1070	3752	5971
like-sign	377	780	448	1605	2573

Table 2: The numbers of dilepton events with at least one secondary vertex reconstructed for the combinations e-e, e-μ and μ-μ, separately for like-sign and unlike-sign leptons. Also indicated is the total number of secondary vertices reconstructed in unlike-sign and like-sign dilepton events.

In order to study Δm_d and Δm_s, the likelihood of the event sample is calculated as a function of these parameters. The construction of the likelihood function follows the procedure described in the previous paper [6]. The true proper time distribution is described by a physics function for each source of events. The B mixing is also described by the physics function. The reconstructed time distributions, $f(t)$, are then obtained by convolving the physics function with resolution functions, $P(t, t')$, which describe the proper time resolution for each source. For example, in the absence of mixing,

$$f(t) = \frac{1}{\tau} \int_0^\infty e^{-\frac{t'}{\tau}} P(t, t') \mathrm{d}t'$$

for a source with lifetime τ. The resolution functions are complicated functions, which must include a description of misreconstruction near $t = 0$, even when the true proper time is large. The probability of this misreconstruction depends on the true proper time, and the description of the resolution function was modified from the previous paper to describe this better. The resolution function has the following form:

$$P(t, t') = C[(1 - \exp(-\frac{t'}{\alpha}))v(t, t') + \exp(-\frac{t'}{\alpha})u(t)]$$

where t and t' are the reconstructed proper time and the true proper time, respectively. The functions $v(t,t')$ and $u(t)$ describe the reconstructed proper time distributions for the correctly reconstructed and misreconstructed vertices respectively. The parameter C is a normalization factor, while α is a parameter to describe the dependence of the misreconstruction probability on the true proper time. Distributions of t and $t-t'$ are shown in Figure 1 for three slices of true proper time t' for Monte Carlo b decays. The fitted resolution function, which is superimposed in the figure, describes the distributions well.

To determine Δm_{d} a three parameter fit is performed, varying Δm_{d} simultaneously with the cascade fraction, the fraction of lepton candidates in $\mathrm{Z} \to \mathrm{b\bar{b}}$ decays that are due to $\mathrm{b} \to \mathrm{c} \to \ell$ decays, and the $\mathrm{B_s^0}$ production fraction, the fraction of b quarks that give rise to $\mathrm{B_s^0}$ mesons. Gaussian constraints reflecting the systematic errors on these two parameters are imposed. The relative uncertainty in the cascade fraction is taken to be $\pm 15\%$ [15], which includes uncertainties due to branching fractions, decay modelling and detector simulation. The $\mathrm{B_s^0}$ production fraction, f_{s}, is constrained both by direct measurements, giving a rate of $(11.1 \pm 2.6)\%$ [3] relative to all weakly decaying b hadrons, and by the measured average mixing rate of b hadrons, $\bar{\chi} = 0.126 \pm 0.008$ [3] together with knowledge of the equivalent parameters, χ_{d} and χ_{s}, for $\mathrm{B_d^0}$ and $\mathrm{B_s^0}$ mesons ($\chi_{\mathrm{d(s)}} = 0.5 \times x^2_{\mathrm{d(s)}}/(1 + x^2_{\mathrm{d(s)}})$). This is equivalent to the constraint $f_{\mathrm{s}} = (11.2^{+1.8}_{-1.9})\%$ [3] except that the values of χ_{d} and χ_{s} are calculated from the values of Δm_{d} and Δm_{s} in the fit, together with the appropriate lifetimes.

In the fit the $\mathrm{B_s^0}$ oscillation parameter is fixed at $\Delta m_{\mathrm{s}} = 10.0\ \mathrm{ps}^{-1}$. The result of the fit is $\Delta m_{\mathrm{d}} = 0.430 \pm 0.045\ \mathrm{ps}^{-1}$. The fitted value of the cascade fraction is 0.078 ± 0.007 compared to the nominal value of 0.066, as calculated from the Monte Carlo sample. The fitted value of f_{s} is $(12.7 \pm 1.9)\%$.

Figure 2 shows the distribution of decay times for all leptons in the dilepton sample and separately for leptons in like-sign and unlike-sign events. The curves are the results of the likelihood fit.

The fraction of like-sign leptons as a function of proper decay time,

$$\mathcal{R}(t) = \frac{N^{LS}(t)}{N^{US}(t) + N^{LS}(t)} ,$$

is plotted in Figure 3 for data, where $N^{LS}(t)$ ($N^{US}(t)$) is the reconstructed time distribution for leptons in like-sign (unlike-sign) events. In the figure, the expected curve for $\Delta m_{\mathrm{d}} = 0.430\ \mathrm{ps}^{-1}$ is shown as the solid line. The fitted values of the cascade fraction and the fraction of leptons from $\mathrm{B_s^0}$ decays are used. Events in which vertices have been reconstructed in both thrust hemispheres enter the plot twice.

4 Systematic Errors on Δm_{d}

In the three parameter fit, the error on Δm_{d} is a combination of statistical error and systematic error due to the constraints on the cascade decay fraction and the $\mathrm{B_s^0}$ production fraction. The systematic error from the cascade decay fraction is estimated by repeating the fit with the central value of the constraint for the cascade fraction changed by +15% or −15% (the systematic uncertainty on this parameter) from its nominal value. The systematic error resulting from the B^0_s production fraction is obtained in a similar way. The statistical error on Δm_d is ± 0.043 ps^{-1}, obtained by subtracting in quadrature these two systematic errors from the fit error.

The uncertainty due to the resolution function description is assessed by repeating the parametrisation using Monte Carlo events in which the tracking resolution is degraded by 10% [22] or improved by 10%. The uncertainty in the background from $Z^0 \to c\bar{c}$ events is taken to be ±30% due to uncertainties in the branching fractions and modelling of semileptonic charm decays, the relative production rates of charmed hadrons, and the uncertainty in the partial width for $Z^0 \to c\bar{c}$. The production rates of B^0_d and B^+ are assumed to be equal and the b-baryon production rate is assumed to lie in the range $(9 \pm 4)\%$. The fraction of D^{**} produced in decays of b hadrons was assumed to be $B(b \to D^{**}) = 0.36 \pm 0.10$. Variations in the efficiency of the secondary vertex reconstruction as a function of decay length are found to have a negligible effect on Δm_d. Uncertainties in the source composition due to Monte Carlo statistics are negligible. The B lifetime variations are performed by changing the ratios of individual B lifetimes while keeping the average lifetime fixed at the LEP, CDF and SLD average value, 1.55 ps^{-1}.

The summary of the sources and estimated values of systematic errors is given in Table 3. The sum of these systematic errors in quadrature is $\delta\Delta m_d =^{+0.028}_{-0.030}$ ps^{-1}.

Source of uncertainty and range	$\delta\Delta m_d$ ps^{-1}
cascade decay fraction (±15%)	−0.010 +0.011
B^0_s fraction (see text)	−0.006 +0.006
resolution function (±10%)	+0.010 −0.010
lepton misidentification (e: ±30%, μ : ±20%)	−0.001 +0.000
charm background (±30%)	−0.006 +0.001
b-baryon fraction (±0.04)	+0.010 −0.009
$B(b \to D^{**})$ (±0.10)	+0.003 −0.003
$\tau_{B^+}/\tau_{B^0_d} = 1.03 \pm 0.06$	+0.019 −0.023
$\tau_{B^0_s}/\tau_{B^0_d} = 1.03 \pm 0.08$	−0.000 +0.001
$\tau_{\Lambda_b}/\tau_{B^0_d} = 0.73 \pm 0.06$	+0.004 −0.004
$\Delta m_s = 2 - 20$ ps^{-1}	+0.004 −0.000
Total systematic error	+0.028 −0.030

Table 3: Summary of systematic errors on the Δm_d measurement. For each source of error, the first error quoted results from varying the parameter in the positive sense.

5 Fit Results for Δm_s

We use the dependence of the likelihood on the assumed value of Δm_s to derive a lower limit. To account for systematic errors when setting the limit, we produce a likelihood curve as a function of Δm_s that includes these effects. This is achieved by maximizing the likelihood with respect to the value of each relevant parameter, constrained by a Gaussian error corresponding to its uncertainty, at each value of Δm_{s}. The constraints are those shown in Table 3. In addition, Δm_{d} is treated as a systematic uncertainty constrained by the average Δm_{d} from analyses using reconstructed D* mesons: $\Delta m_{\mathrm{d}} = 0.52 \pm 0.05$ ps^{-1} [4, 5]. The exception to this scheme is the treatment of the resolution function description. In this case, three curves of $\ln \mathcal{L}$ were calculated, including all other systematic uncertainties, assuming the default tracking resolution or assuming the tracking resolution was degraded or improved by 10%. The smallest of the three values of $-\Delta \ln \mathcal{L}$ was taken at each value of Δm_{s}. The solid curve in Figure 4 shows the difference in log-likelihood from the maximum as a function of Δm_{s} with systematic errors included.

We set the limit on the basis of the difference in log-likelihood, $\Delta \ln \mathcal{L}$, with respect to the maximum value. A Monte Carlo technique was used to determine the correspondence between confidence levels and values of $\Delta \ln \mathcal{L}$ as a function of Δm_{s}. This approach is found to be more reliable than the approach of the previous paper [6], where $-\Delta \ln \mathcal{L} = 1.92$ was assumed to correspond to 95% confidence level. Many data sets, of the same size as the real data sample, were simulated using a fast Monte Carlo and fitted in a manner similar to the data. The main systematic errors affecting the Δm_{s} result were simulated by allowing the parameters of the Monte Carlo to vary independently for each data set. The corresponding parameters were allowed to vary under Gaussian constraints in the fit. The exception to this was the parameter governing the proper time resolution, which was treated in the same way as in the data fit. For each simulated data sample a single value of $\Delta \ln \mathcal{L} = \ln \mathcal{L}_{\mathrm{max}} - \ln \mathcal{L}(\Delta m_{\mathrm{s}}^*)$ was extracted, where Δm_{s}^* is the generated value of Δm_{s}. The $\Delta \ln \mathcal{L}$ corresponding to 95% confidence was defined to be that value above which lay only 5% of the simulated data samples. This procedure was performed for input values of $\Delta m_{\mathrm{s}}^* = 1.0, 2.0, 4.0$ and 8.0 ps^{-1}, using 3000 Monte Carlo data sets at each value of Δm_{s}^*. The results of this study are shown as the dashed line in Figure 4. We exclude the region of $\Delta m_{\mathrm{s}} < 2.2$ ps^{-1} at 95% C.L.

To assess the importance of the systematic errors, we studied the log-likelihood as a function of Δm_{s}, while fixing all other parameters. These parameters were set to the values that maximized the log-likelihood at the preferred value of Δm_{s} in the procedure described above. The result is shown as the dotted curve in Figure 4. We conclude that the systematic errors have only a minor effect on our result.

Using the data sets simulated with the fast Monte Carlo referred to above, we were able to check the analysis technique and study the expected sensitivity to Δm_{s}. The results of these studies are shown in Figure 5. Each row corresponds to a different generated value of Δm_{s}, indicated by the Δm_{s}^* at the right edge of the plot. The left column shows the fitted value of Δm_{s} for each trial. In the right column are normalised cumulative distributions of the log-likelihood difference between the value at the fitted maximum and the value at the generated Δm_{s} for each trial. The sensitivity of this analysis is good for $\Delta m_{\mathrm{s}}^* < 4$ ps^{-1}, but is lost between 4 ps^{-1} and 8 ps^{-1}.

6 Conclusion

We have measured the oscillation frequency $\Delta m_{\rm d}$ by measuring the proper time of B meson decays and tagging the charges of leptons in both thrust hemispheres. The $\rm B^0_d - \bar{B}^0_d$ oscillation parameter is measured to be:

$$\Delta m_{\rm d} = 0.430 \pm 0.043 \ {}^{+0.028}_{-0.030} \ \rm ps^{-1} \ ,$$

corresponding to $(2.83 \pm 0.28^{+0.18}_{-0.20}) \times 10^{-4}$ eV. This result is consistent with and supersedes the result using 1991-1993 data.

The $\Delta m_{\rm d}$ value is consistent with the OPAL results $\Delta m_{\rm d} = 0.548 \pm 0.050 \ {}^{+0.023}_{-0.019} \ \rm ps^{-1}$ [5] from data containing $\rm D^{*\pm}$ mesons and leptons, and $\Delta m_{\rm d} = 0.444 \pm 0.029 \ {}^{+0.020}_{-0.017} \ \rm ps^{-1}$ [7] from inclusive lepton events. Combining these results, taking into account correlations in the systematic errors, we find

$$\Delta m_{\rm d} = 0.467 \pm 0.022 \ {}^{+0.017}_{-0.015} \ \rm ps^{-1} \ .$$

The small statistical correlations between the results were found to have a negligible effect. This result is consistent with previous measurements [4, 8]. Using $\tau_{\rm B^0_d} = 1.56 \pm 0.06\,\rm ps$, the combined OPAL value gives $x_{\rm d} = 0.73 \pm 0.04 \pm 0.03$, where the last error is due to the uncertainty in $\tau_{\rm B^0_d}$. This value is also consistent with the average of ARGUS and CLEO measurements, $x_{\rm d} = 0.67 \pm 0.08$ [2, 3].

We obtain a lower limit on $\Delta m_{\rm s}$ at 95% confidence level: $\Delta m_{\rm s} > 2.2 \ \rm ps^{-1}$. This limit is less constraining than the ALEPH results[8, 9] and a recent OPAL result [7].

Acknowledgements

We particularly wish to thank the SL Division for the efficient operation of the LEP accelerator and for their continuing close cooperation with our experimental group. We thank our colleagues from CEA, DAPNIA/SPP, CE-Saclay for their efforts over the years on the time-of-flight and trigger systems which we continue to use. In addition to the support staff at our own institutions we are pleased to acknowledge the
Department of Energy, USA,
National Science Foundation, USA,
Particle Physics and Astronomy Research Council, UK,
Natural Sciences and Engineering Research Council, Canada,
Israel Science Foundation, administered by the Israel Academy of Science and Humanities,
Minerva Gesellschaft,
Benoziyo Center for High Energy Physics,
Japanese Ministry of Education, Science and Culture (the Monbusho) and a grant under the Monbusho International Science Research Program,
German Israeli Bi-national Science Foundation (GIF),
Direction des Sciences de la Matière du Commissariat à l'Energie Atomique, France,

Bundesministerium für Bildung, Wissenschaft, Forschung und Technologie, Germany,
National Research Council of Canada,
Hungarian Foundation for Scientific Research, OTKA T-016660, T023793 and OTKA F-023259.

References

[1] See for example: P. Franzini, Physics Reports **173** (1989) 1.

[2] ARGUS Collaboration, H. Albrecht *et al.*, Z. Phys. **C 55** (1992) 357;
ARGUS Collaboration, H. Albrecht *et al.*, Phys. Lett. **B 324** (1994) 249;
CLEO Collaboration, J. Bartelt *et al.*, Phys. Rev. Lett. **71** (1993) 1680.

[3] Particle Data Group, 'Review of Particle Physics', Phys. Rev. **D 54** (1996) 1.

[4] ALEPH Collaboration, D. Buskulic *et al.*, Phys. Lett. **B 313** (1993) 498;
DELPHI Collaboration, P. Abreu *et al.*, Phys. Lett. **B 338** (1994) 409;
DELPHI Collaboration, P. Abreu *et al.*, Z. Phys. **C 72** (1996) 17;
L3 Collaboration, M. Acciarri *et al.*, Phys. Lett. **B 383** (1996) 487;
ALEPH Collaboration, D. Buskulic *et al.*, CERN-PPE/96-102, submitted to Z. Phys. C.

[5] OPAL Collaboration, G. Alexander *et al.*, Z. Phys. **C 72** (1996) 377.

[6] OPAL Collaboration, R. Akers *et al.*, Z. Phys. **C 66** (1995) 555.

[7] OPAL Collaboration, K. Ackerstaff *et al.*, CERN-PPE/97-36, submitted to Z. Phys. C.

[8] ALEPH Collaboration, D. Buskulic *et al.*, Phys. Lett. **B 322** (1994) 441.

[9] ALEPH Collaboration, D. Buskulic *et al.*, Phys. Lett. **B 356** (1995) 409;
ALEPH Collaboration, D. Buskulic *et al.*, Phys. Lett. **B 377** (1996) 205.

[10] Y. Nir, Phys. Lett. **B 327** (1994) 85;
A. Ali and D. London, Z. Phys. **C 65** (1995) 431.

[11] OPAL Collaboration, K. Ahmet *et al.*, Nucl. Inst. and Meth. **A 305** (1991) 275.

[12] P. Allport *et al.*, Nucl. Inst. and Meth. **A 324** (1993) 34;
P. Allport *et al.*, Nucl. Inst. and Meth. **A 346** (1994) 476.

[13] OPAL Collaboration, G. Alexander *et al.*, Z. Phys. **C 52** (1991) 175.

[14] OPAL Collaboration, R. Akers *et al.*, Z. Phys. **C 63** (1994) 197.
The jet finding parameters ϵ and R are set to 5.0 GeV and 0.65, respectively.

[15] OPAL Collaboration, P. Acton *et al.*, Z. Phys. **C 58** (1993) 523.

[16] OPAL Collaboration, R. Akers *et al.*, Z. Phys. **C 60** (1993) 199.

[17] T. Sjöstrand, Comp. Phys. Comm. **82** (1994) 74.

[18] OPAL Collaboration, G. Alexander *et al.*, Z. Phys. **C 69** (1996) 543.

[19] J. Allison *et al.*, Nucl. Instrum. Methods **A 317** (1992) 47.

[20] C. Peterson, D. Schlatter, I. Schmitt and P. Zerwas, Phys. Rev. **D 27** (1983) 105.

[21] D. Bardin *et al.*, *ZFITTER, An Analytical Program for Fermion Pair Production in* e^+e^- *Annihilation*, CERN-TH/6443-92.
For this prediction, the Z^0, top quark, and Higgs boson masses are set to $M_{Z^0} = 91.18$ GeV, $M_{\rm top} = 150$ GeV and $M_{\rm Higgs} = 300$ GeV, and $\alpha_s = 0.12$.

[22] OPAL Collaboration, R. Akers *et al.*, Z. Phys. **C 65** (1995) 17.

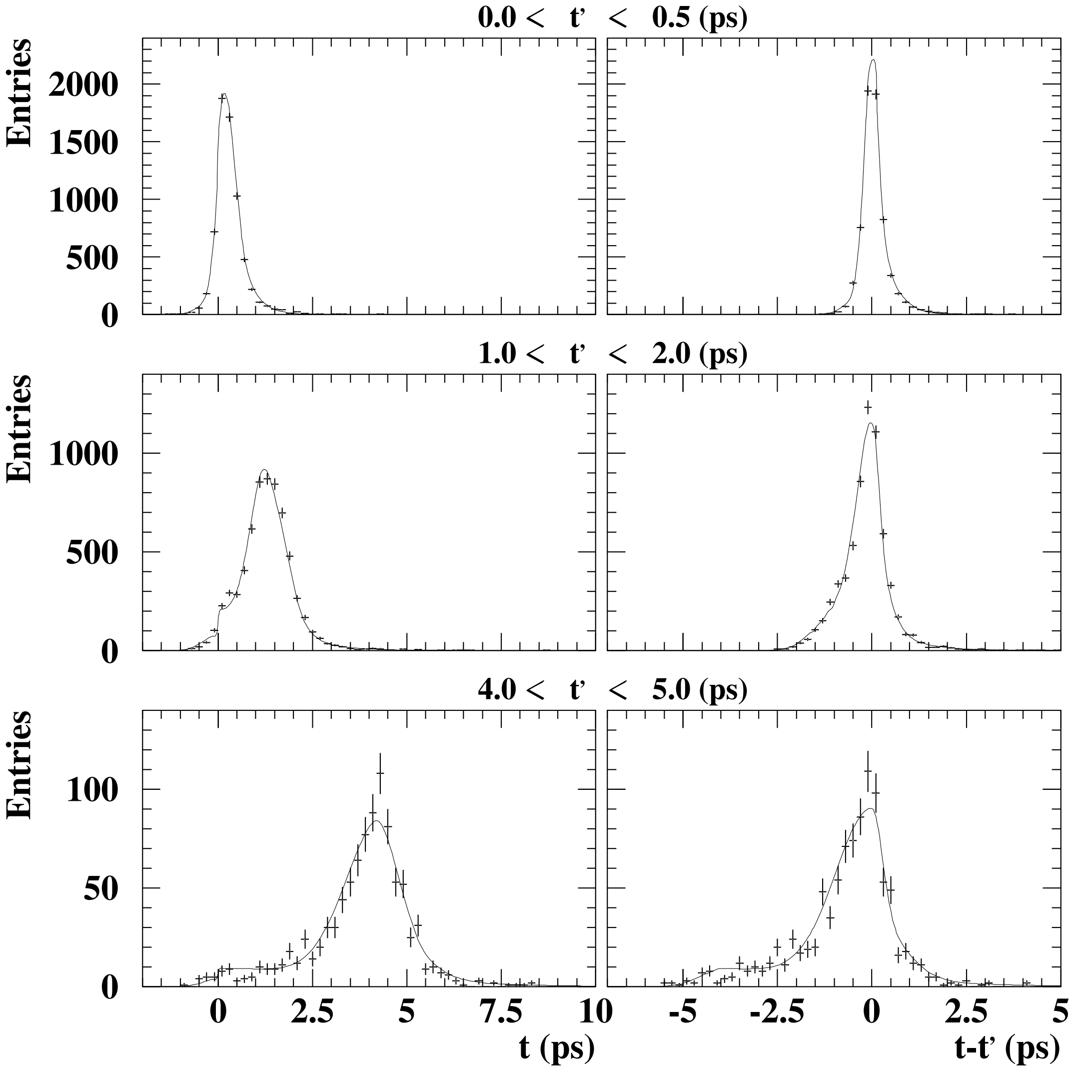

Figure 1: The distributions of reconstructed proper time, t, and $t - t'$ in three slices of the true proper time t' for leptons from primary b hadron decays in the Monte Carlo. Also shown is the parametrisation of these distributions.

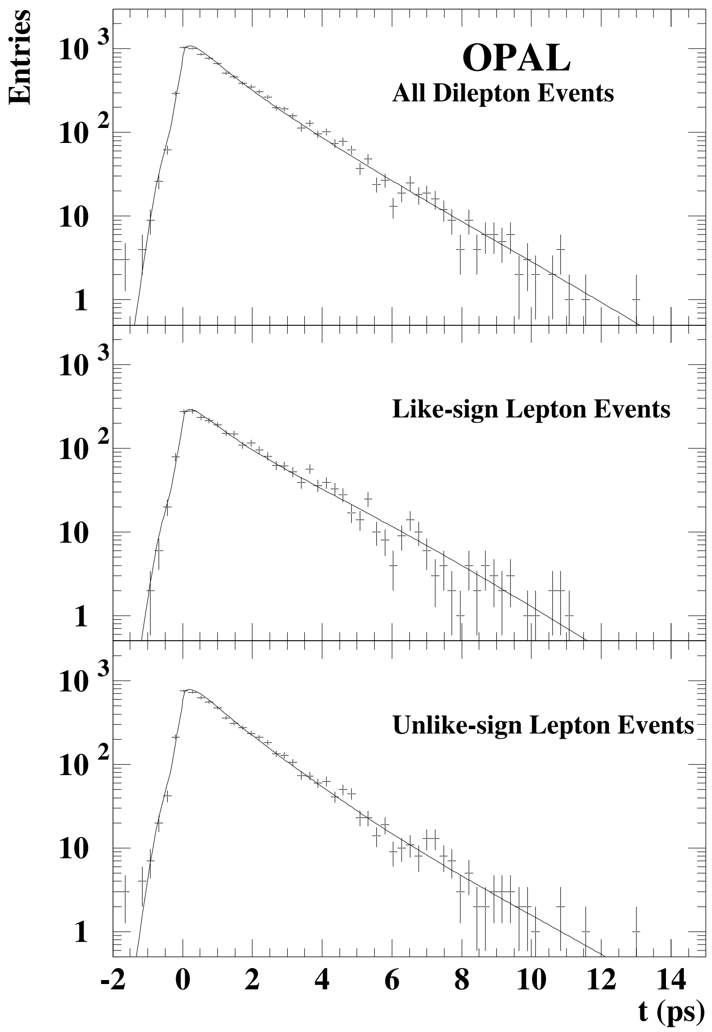

Figure 2: The proper time distributions for all leptons in dilepton events (top) for which a vertex is found, and for those leptons in like-sign (centre) and unlike-sign (bottom) events. The curves represent the results of the maximum likelihood fit.

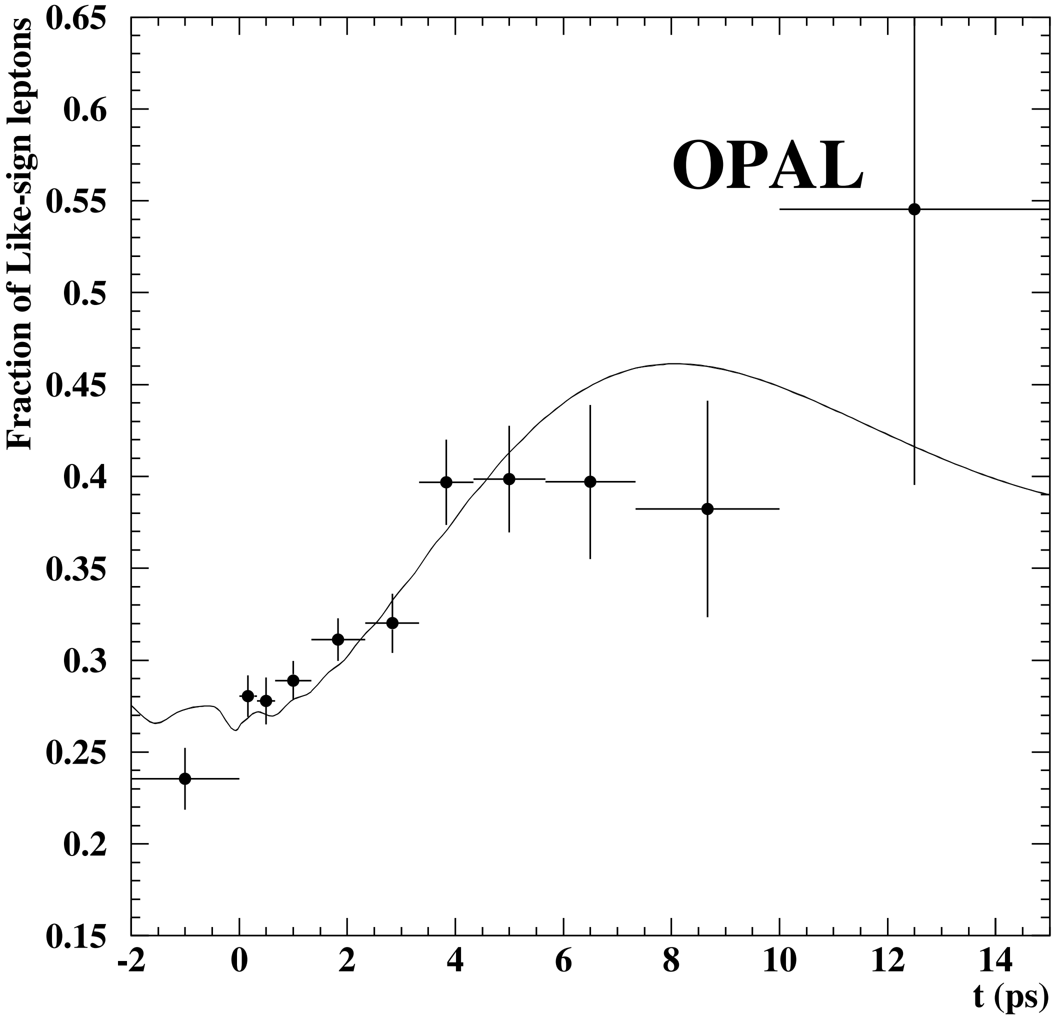

Figure 3: The fraction of like-sign leptons as a function of proper decay time: $\mathcal{R}(t)$. The solid curve represents the expectation with Δm_{d} set to 0.430 ps^{-1} and Δm_{s} set to 10.0 ps^{-1}.

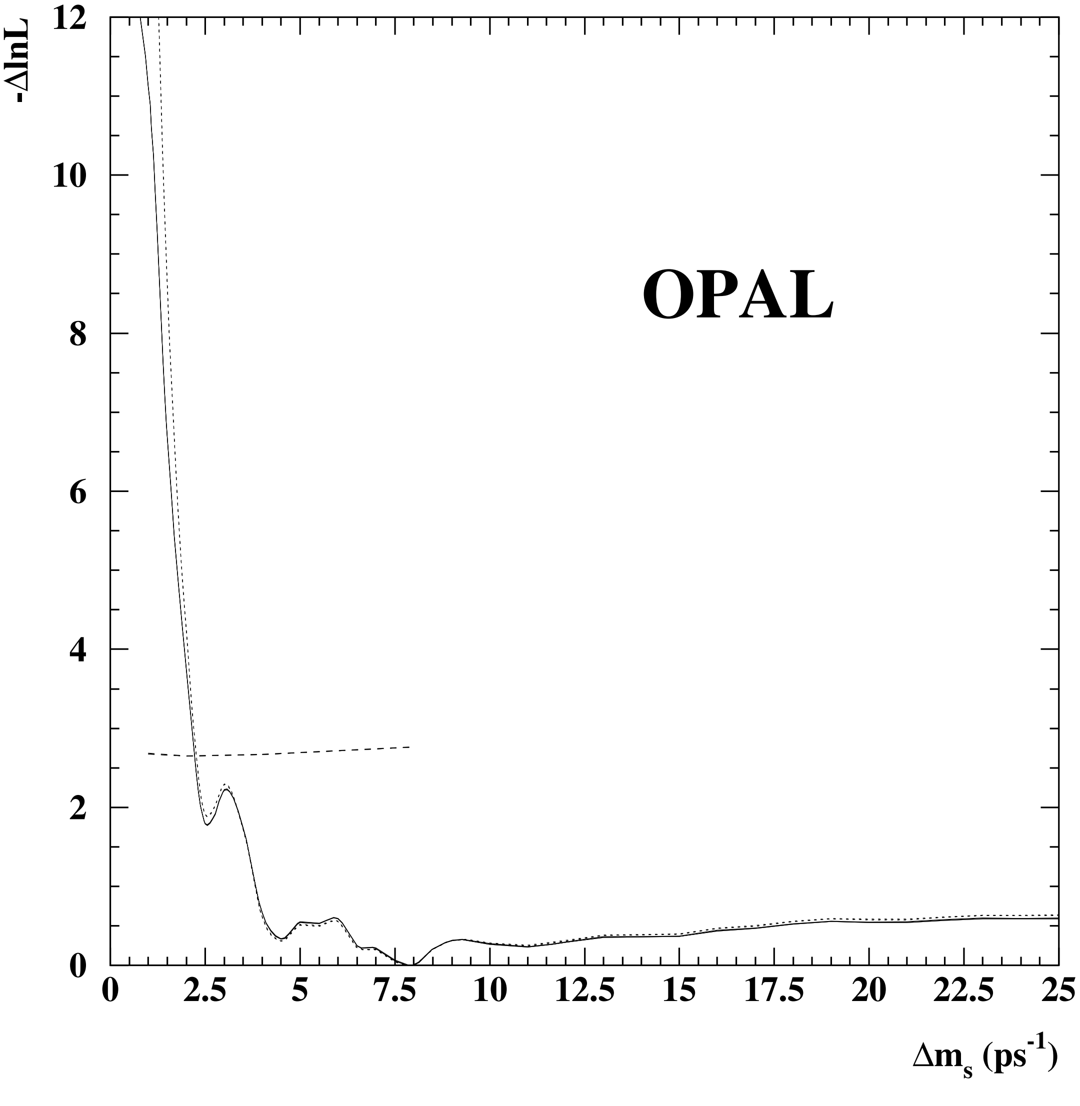

Figure 4: The difference in log-likelihood from the maximum value is shown as a function of Δm_s. The solid curve includes the effect of systematic errors, while the dotted curve includes only statistical errors. The dashed curve shows the 95% C.L.

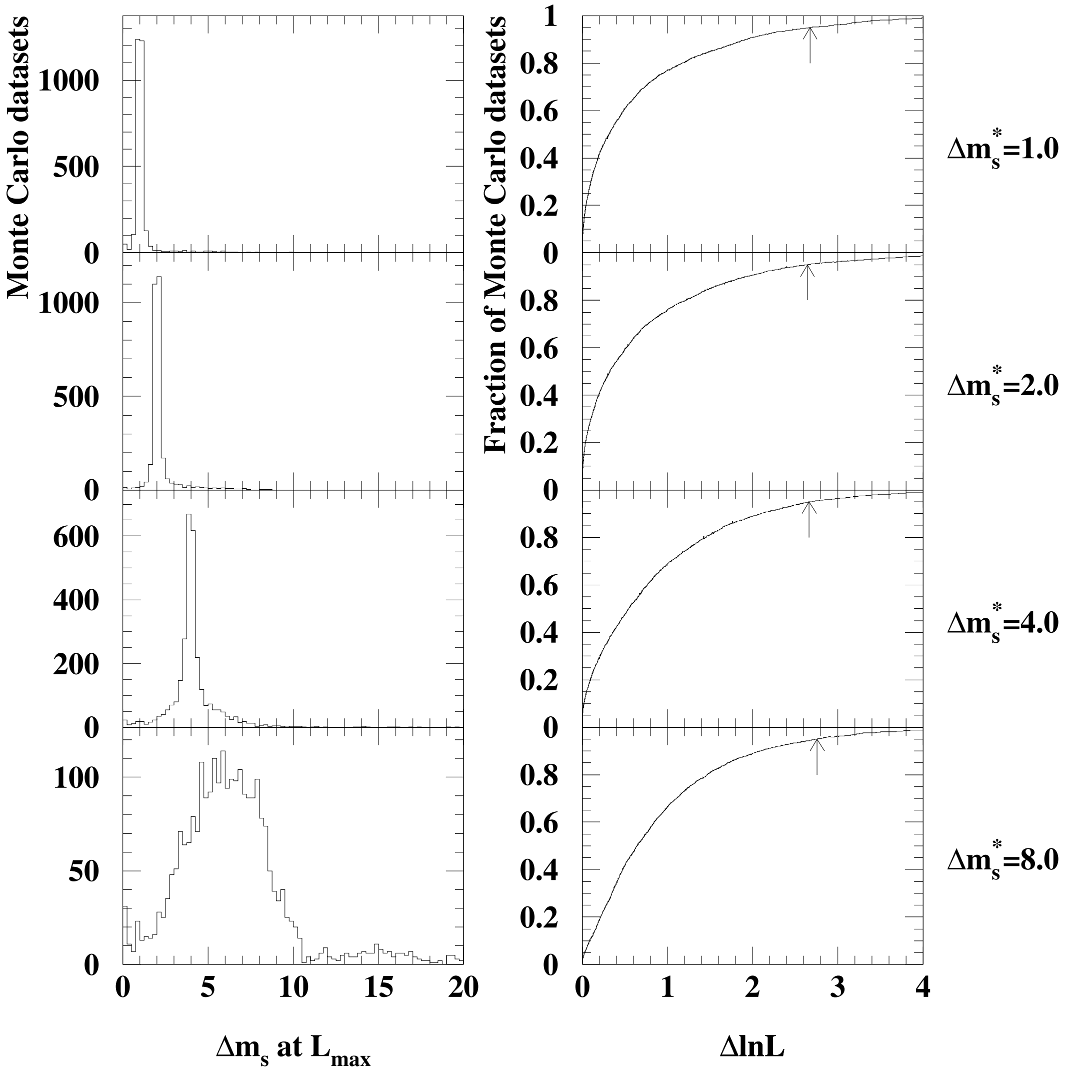

Figure 5: The results of fits to 3000 toy Monte Carlo datasets are shown. The Δm_s^* value indicates the generated value of Δm_s in ps^{-1}. The left-hand column shows the distribution of fitted values of Δm_s for each Δm_s^* value. The right-hand column shows the normalised cumulative distribution of the difference between the log-likelihood values at the fitted maximum and at the generated value. The arrow indicates the 95% confidence level value.